Jurnal Tribologi 29 (2021) 11-30

Jurnal Tribologi
Website : jurnaltribologi.mytribos.org e-issn: 2289-7232

Mechanical and tribological properties of FFF 3D-printed polymers: A brief review

Mohamad Nordin Mohamad Norani [1], Muhammad Ilman Hakimi Chua Abdullah [2,3*], Mohd Fadzli Bin Abdollah [1,3], Hilmi Amiruddin [1,3], Faiz Redza Ramli [1,3], Noreffendy Tamaldin [1,3]

[1] Fakulti Kejuruteraan Mekanikal, Universiti Teknikal Malaysia Melaka, Hang Tuah Jaya, 76100 Durian Tunggal, Melaka, MALAYSIA.
[2] Fakulti Teknologi Kejuruteraan Mekanikal dan Pembuatan, Universiti Teknikal Malaysia Melaka, Hang Tuah Jaya, 76100 Durian Tunggal, Melaka, MALAYSIA.
[3] Centre for Advanced Research on Energy, Universiti Teknikal Malaysia Melaka, Hang Tuah Jaya, 76100 Durian Tunggal, Melaka, MALAYSIA.
*Corresponding author: ilmanhakimi@utem.edu.my

KEYWORDS

Polymer
3D printer
Mechanical
Tribological

ABSTRACT

In fused filament fabrication (FFF); the process of 3D printing using polymer-based materials; specialised and functional parts are designed and manufactured for use in engineering and medical industries. Recognizing the impact on the mechanical and tribological behaviour of different processing parameters, composite materials, internal geometries, and lattices will allow a better understanding of the characteristics of FFF end-products. However, obtaining this information proves to be complicated. The review of current literature and research related to the use in real-life applications is therefore essential, as this will not only help to identify valuable characteristics, vital processing parameters, and limitations, but will also help to understand the results of these studies. As such, a systematic and classification-based literature review was performed on the mechanical and tribological properties of 3D-printed polymers.

1.0 INTRODUCTION

At present, industries are focusing on shortening the time taken to develop and manufacture a product in order to ensure faster market entry and meet the ever-increasing demands. According to ASTM52900-15 (2015), this can be accomplished with the help of rapid prototyping

Received 21 December 2020; received in revised form 9 March 2021; 18 April 2021.
To cite this article: Norani et al., (2021). Mechanical and tribological properties of FFF 3D-printed polymers: A brief review. Jurnal Tribologi 29, pp.11-30.

technologies (RPT); also known as additive manufacturing (AM). In AM, a 3D-model is first designed using computer-aided design (CAD) software and saved in stereolithography (STL) file format before the product is finally fabricated layer-by-layer. This method is also used in additive layer manufacturing, layered manufacturing, additive fabrication, additive techniques, additive processes, and solid freeform fabrication (Hull., 1986). The successful manufacturing of materials for use in wear and friction applications are a primary concern for bearings as it is an essential component in friction assemblies that operate inside vehicles, textile machinery, food processing machinery, and machines used in the chemical industry (Vishnu et al., 2020).

Fused filament fabrication (FFF) is an additive manufacturing (AM) process that is typically used in 3D printing applications. It is a method of manufacturing via extrusion, where the material is dispensed via a nozzle. To be more specific, the hydrogen molecules and Van der Waals forces within a polymer are temporarily broken when it is heated to a liquid state but is re-established once the polymer is injected through the nozzles and it cools and hardens (Peças et al., 2018). At present, 3D-printed pieces are currently used to design visual aids, demonstration templates, and other components. On the other hand, FFF is being used in the manufacturing sector for the rapid production of goods (Aslanzadeh et al., 2018; Liu et al., 2019; Sabahi et al., 2020; Jasiuk et al., 2018). However, its suitability and stability towards mechanical loading need to be thoroughly examined before it can be used in diverse applications.

Over the years, AM techniques have expanded to fused deposition modelling (FDM), stereolithography (STL), powder bed and inkjet head 3D printing, selective laser sintering (SLS), selective laser melting (SLM), direct metal laser sintering (DMLS), and laminated object manufacturing (LOM) (Prakash et al., 2018). These technologies are being used more often because it allows different materials to be embedded in various applications to manufacture highly complex geometric parts. In contrast to AM, a single component cannot be manufactured using conventional methods such as cutting and casting due to machine limitation (Hiroaki et al., 2019). In addition, 3D components are now used to make the final product, otherwise used to develop the prototype in the early manufacturing process (Tibbits, 2003; Chua et al., 2014). In the field of medical education, the application helps to build identical biological and virtual model material with each slice of contour organ and completed joined part (Seliktar et al., 2012; Huang et al., 2013; Chua et al., 2015 and Murphy et al., 2014). In the case of civil construction, the 3D printing can now safely time and transform architecture even better in the design of building contoursto reduce theenvironmental construction waste (Hager et al., 2016). Furthermore, their versatility in the use ofplastics, alloys, composites, ceramics, polymers, biomaterials, and concrete also provide the most vital advantage of material savings and strength.

There are three FFF method parameters; 1) slicing: where the nozzle diameter/bead width, layer thickness/height, flow rate, deposition speed, raster orientation/angle, infill, air gaps between, raster pattern, number of contour width, top and bottom thickness are determined, 2) orientation: which is commonly horizontal or vertical, or lateral in the case of research specimens, although other print angle orientations may also be used, and 3) the temperature at which to print test specimens, the extrusion temperature, or the bed platform temperature (Mohamed et al., 2015). This FFF method parameter better presented in Figure 1.

Figure 1. FFF method parameters.

Many materials are being used in FFF technologies, and the most commonly utilised materials are thermoplastics and thermosets. While thermoplastics are recyclable, tough, and easily repaired with solvent, thermosets have good chemical and thermal resistance but are non-recyclable and brittle (Sreenivasan et al., 2013). Thermosets and thermoplastics have different

characteristics and chemical structures than metal powders and natural fibres. They are still extremely versatile as they can be fabricated into various complex shapes and possess impressive viscous properties and are low cost and easy to manufacture. However, thermoplastics are stronger than thermosets as they can absorb higher impact energies (Furtado et al., 2012). Due to this, and the abovementioned reasons, thermoplastics are a suitable replacement for thermosets in the manufacturing industry. The most commonly used thermoplastic filaments are acrylonitrile butadiene styrene (ABS) and polylactic acid (PLA). The characteristics of both thermosets and thermoplastics are tabulated in Table 1 (Kabir et al., 2012). This paper also focuses on other materials; such as polycarbonate (PC), ABS + hydrous magnesium silicate composite, carbon fibre reinforced ABS (CFRABS), polyetherimide (PEI, Ultem®), polyether ether ketone (PEEK), Nylon 12 polyamide (PA12), polytetrafluoroethylene (PTFE), and polyurethane (PU).

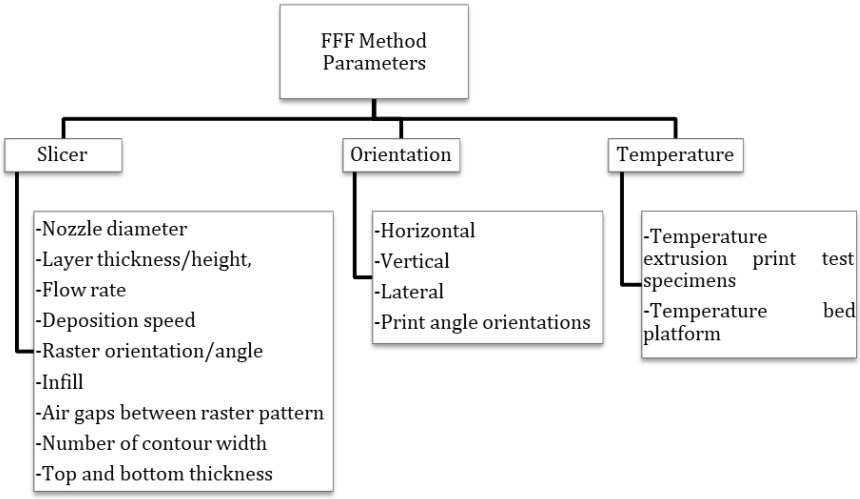

Figure 1: FFF method parameters.

Table 1: Differences between thermosets and thermoplastics (Kabir et al., 2012).

Polymers	**Thermoplastics**	**Thermosets**
Advantages	-Recyclable -Post-formable -Easy to restore/repair via welding or solvent bonding -Tough	-Low-viscosity resin -Excellent thermal stability once polymerised -Good fibre wetting -Chemically resistant
Disadvantages	-Must be heated past freezing point for processing purposes	-Non-biodegradable via standard techniques -Brittle -Not post-formable -Poor melt flow

The ultimate goal in mechanical engineering is to extend the lifespan of machine parts while reducing wear and tear from friction. While the mechanical properties of a material affect the load-bearing behaviour, the elastic modulus influences the load-bearing rate of deflection.

Moreover, the strength determines the amount of force that the material can withstand before failure, and the ductility determines when the material fails once the elastic threshold is exceeded. This is because all mechanical properties respond only to loads during operation. Examples of mechanical properties are elastic modulus, tensile strength, elongation, hardness, and fatigue limit. For tribological properties, friction and wear are dependent on resistance during sliding contact. Optimising and reducing friction and wear not only improves energy efficiency but also ensures a longer service life. With this mechanical and tribological information, the user will have quicker solutions for repairing damaged components by fabricating parts remotely or making on-demand modified objects (Hiroaki et al., 2019; Soffie et al., 2020; Mohd et al., 2020). As such, the mechanical properties of manufactured parts have become an important factor in the manufacturing industry. Therefore, the mechanical and tribological properties of 3D-printed polymers warrant evaluation in terms of printing parameters, composite materials, internal geometries, lattices, and optimisations.

2.0 MECHANICAL PROPERTIES

The purpose of this section is to provide researchers and FFF users with valuable information before they purchase a 3D printer or material. It provides studies that demonstrate a connection between mechanical properties and processing parameters as well as the optimal parameter settings from different mechanical property viewpoints. As previously mentioned, FFF processing parameters significantly affect mechanical properties; particularly the small layer thickness, negative raster to raster air gap, raster angle, construction orientation, and 100% infill percentage to increase strength. The correlation between these parameters plays a crucial part in the mechanical properties (Tymrak et al., 2014; Rankouhi et al., 2016). As such, several researchers developed a rank-based categorisation of the parameters. For instance, Kim et al., (2017) state that multiple materials significantly influence mechanical properties than single materials.

Tymrak et al. (2014) studied the mechanical properties of components fabricated with open-source 3-D printers and found that a layer height of 0.2 mm resulted in a better strength compared to layer heights of 0.4 mm and 0.3 mm. They also found the average tensile strength of ABS and PLA to be 28.5 MPa and 56.6 MPa, respectively, while the average elastic moduli were 1807 MPa and 3368 MPa, respectively. This was due to high temperature of the extruder and filament, which created significant thermal bonding between both the raster and the layers, leading to greater fusing. Rankouhi et al., (2016) concluded that the layer thickness and raster orientation should be as low as possible to improve the mechanical strength and the small airgap to material ratio is the main factor contributing to higher strength. Therefore, a minimum layer thickness produces higher tensile strength and elastic modulus due to smaller fusing gaps between the thermal interlayers.

The Infill percentage 3D parameter contributes significantly to mechanical strength. For example, Samykano et al., (2019) found that ABS had the highest tensile strength of 33.78 MPa at a layer height of 0.5 mm, raster angle of 55°, and infill density of 80%. The same parameters also yielded the maximum elastic modulus of 787.68 MPa. For 3D-printed PLA, the maximum strength was at filling factors of 100% (Perepelkinaa et al., 2020). This was probably due to fill porosity, low adhesion between the plastic layers, and stretching of molecular bonds as it is unable to stretch due to the initial stage appearance of cross-bridges which gives a low binding energy. As a result, the polymer was brittle. Therefore, higher fill percentage increased the strength and viscosity due to the formation of adhesive bonds between molecules.

Kim et al., (2017) investigated the mechanical properties of single and dual-material 3D-printed products using PLA and ABS filaments via full factorial design of experiment (DOE) and analysis of variance (ANOVA). The investigation was performed by varying the infill percentages at 50% and 100% with orientation directions of x-axis, y-axis, and 45° angle. The findings showed that dual-material 3D-printed products have an average ultimate tensile strength of 43.26 MPa compared to single-material 3D-printed products. 3D-printed materials using PLA in the x-direction and with an infill percentage of 100% gave the best mechanical properties with a surface roughness of 1.938 μm. Moreover, the orientation direction in AM samples contributed to its anisotropic properties (Ahn et al., 2002). Hence, these infill and orientation direction factors improved the mechanical properties of 3D-printed products making them more rigid and firm.

The compressive effect of internal structures and pattern on mechanical properties was examined by Galeta et al., (2016). A honeycomb structure (H) 3D-printed along the y-axis in a plaster-based powder zp130, with an appropriate binder zb56 (Z310 printer) had a maximum tensile strength of 13.92 MPa. The maximum (1.78 MPa/g) and minimum (0.21 MPa/g) results of specific tensile strengths at failure break were achieved in the same honeycomb data set. Similarly, Domínguez-Rodríguez (2018) examined the 3D-printed structures filled with honeycomb patterns in the longitudinal direction (0/90 40%) and found that the honeycomb structure had the most effective stiffness and strength properties compared to rectangular patterns. The combination of local plastic deformation and buckling between interchange layers contributed significantly to the properties (Gibson et al., 1991).

Some researchers have used the DOE, Taguchi, Box–Behnken Design (Soffie et al., 2020), and ANOVA methods to optimise the mechanical properties and the after-effect relationships. These are known systematic methods that use statistical data to determine the correlation between factors affecting a process and its output (cause-and-effect). Sood et al., (2010) used MINITAB R14® face-centred central composite design (FCCCD) to study the effect of five important processing parameters; 1) layer thickness, 2) orientation, 3) raster angle, 4) raster width, and 5) air gap on three responses; 1) tensile, 2) flexural, and 3) impact strength of an ABS P400 test specimen. A layer thickness 0.1270 mm, 0° orientation, 60° raster angle, 0.4064 mm raster width, 0.0080 mm air gap was found to yield the maximum tensile strength, flexural strength, and impact strength at 17.92 MPa, 37.80 MPa, and 0.93 Mj/m^2, respectively. This is because flexural testing creates low strength interactions between 2D-laminates or delaminated layers prior to the breakdown of 2D laminates or layers. Delamination is also seen in layered fabrics, with differences in pressure (Lee et al., 2007). Onwubolu and Rayegani (2014) examined ABS mechanical properties via characterisation and optimisation using DOE and group method of data handling (GMDH). They found that minimum layer thickness, part orientation of zero, maximum raster angle and raster width, and negative air gap produced the highest tensile strength.

Multiple studies have investigated the process parameters of composites (Christiyana et al., 2016, Nor et al., 2018, Ahn et al., 2002). Christiyana et al., (2016) experimentally studied the influence of process parameters on the mechanical properties of a 3D-printed ABS + hydrous magnesium silicate composite. Samples with a layer thickness of 0.2 mm and printed at a low speed of 30 mm/s had the highest tensile strength (28 MPa) and flexural strength (45 N). As Es-Said et al., (2000) proposed, this could be due to weak interlayer attachment or porosity in AM samples. The effect of layer thickness and fill angle on ABS and carbon fibre reinforced ABS (CFRABS) materials was explored by Nor et al., (2018) using the Taguchi method, signal-to-noise (S/N) ratio analysis, and ANOVA. The optimal tensile stress parameters were found at 0.18mm of layer thickness, 90° of fill angle with 32.526 MPa for ABS and 21.619 MPa for CFRABS.

In general, owners of 3D printers need to familiarise themselves with the mechanical properties of their materials prior to manufacturing components. When working with a different type of polymer, the 3D printer will require a different parameter setting, filling pattern, internal geometry, and lattice structure which will influence the final component's mechanical properties. Azmi et al., (2018) examined the correlation between the compressive strength performance and the dynamic behaviour of a strut diameter lattice structure via vibration analysis. The compression test results indicate that an increase in strut diameter size could increase compressive strength performance (0.8MPa) and provide better energy absorption. It was also found that increasing the strut diameter to 1.6 mm significantly increased the Young's modulus and lattice structure; 23% and 69% compared to strut diameters of 1.4 mm or 1.2 mm respectively.

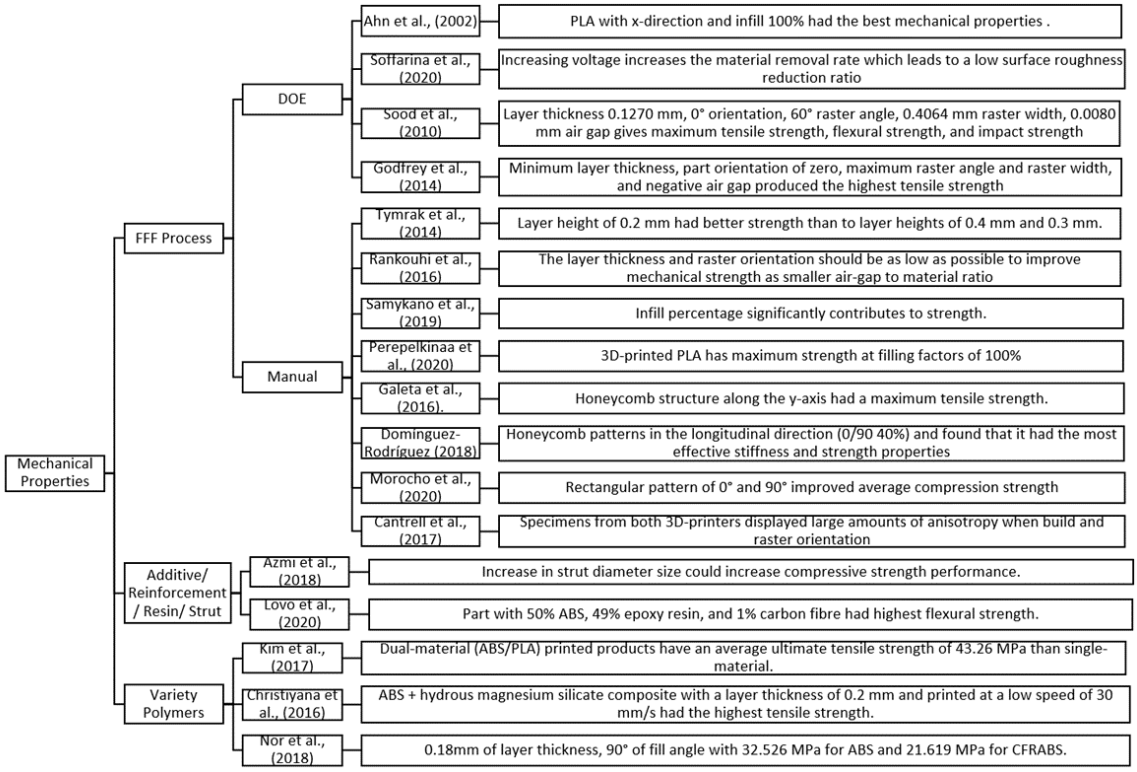

Figure 2: Research map (mechanical properties).

Morocho et al., (2020) subjected rectangular and hexagonal filled ABS polymers to mechanical compression tests and found that these structures improved the mechanical properties of 3D-printed parts and increased tensile strength because of the- internal structures' geometric arrangements. In addition, a rectangular fill pattern of 0° and 90° was also found to improve mechanical properties in terms of the average compression strength (33.147MPa) and the percentage of deformation (5.96%). Lovo et al., (2020) attempted a new mechanical design technique that combined the high geometry flexibility of AM with a structured internal geometry filled and reinforcement material. Results after optimisationshowed that the part with 50% ABS,

49% epoxy resin, and 1% carbon fibre had a flexural strength of 112 MPa. Moreover, the 3D-printed ABS, without resin reinforcement, had a dense specific weight of 110% from 1.1 g/cm^3.

Cantrell et al., (2017) provided an experimental characterisation of the mechanical properties such as tensile strength and shear characterisation of 3D-printed ABS and polycarbonate (PC) parts. The degree of anisotropy present in 3D-printed materials was determined by printing the specimens with changing rasters (+45/-45, +30/-60, +15/-75 and 0/90) and build concentrations (flat, on-edge, and up-right). The shear modulus and shear yield strength of the ABS specimen varied by up to 33%. The raster orientations in the flat-built PC specimens displayed anisotropic behaviour as the modulus and strengths gone up to 20%. Those all researchers are shown in Figure 2 (researcher map). Table 2 provides an overview of other similar findings on the mechanical properties of 3D-printed polymer parts.

Table 2: Summary of studies on the mechanical properties of polymers.

Authors	**Research Objective**	**Polymer Material**	**Method**	**Findings**
Uddin M et al., 2017	Compressive and tensile strength	ABS	Layer thickness: 0.39 mm, 0.19 mm, 0.09 mm Printing plane: XY, YZ, ZX Printing orientation: vertical, horizontal, diagonal	The highest Young's modulus (1524 MPa) was found at layer thickness 0.09 mm, printing plane YZ, horizontal orientation among all the 3D-printed tensile specimens. Compression test results indicate that printing plane XY with horizontal orientation and printing plane XY with diagonal orientation yielded the highest stiffness and yield strength.
Seidl M et al., 2017	Flexural and tensile strength	ABS	Printer type Building orientation: 0°, 45°, 90°	Highest tensile modulus (2294 MPa) and flexural modulus (2247 MPa) achieved by specimens 3D-printed using Fortus 450 at 90°.
Balderrama-Armendariz CO et al., 2018	Torsional forces	Stratasys ABS-M30™	Print orientation: XYZ, YXZ, XZY, ZXY Raster angle: 0°, 45°, 90°, 45°/45°	Specimen with YXZ orientation and 0 ° raster angle had highest fracture strain and ultimate strength.
Leite M et al., 2018	Water absorption capacity, compression, and tensile strength	ABS	Build direction: Y, Z, Raster angle: 0°/90°, 45°/–45°, 0°, 90°, 45°, – 45°	Specimen with Z build direction and 0°/90° raster angle had higher water absorption (0.015 gcm^2). Specimen with 45° raster angle had higher compression modulus (800.3 MPa) and tensile modulus (849.3 MPa).
Quan et al., 2018	Compression	Polyoxymethylene (POM),	Part structure: solid cube, 3D braid	Solid cube: interlayer delamination/crack occurred in 0°- and 45°-direction specimens at a strain

		POM + 30% glass fibres (GF), POM + 20% PTFE, Polyamide 6.6 (PA6.6), PA6.6 + 30% GF, ultra-high molecular weight polyethylene (PE)	Printing direction: 0°, 45°, Z	level of around 25%, the difference in stress-strain relationships was not significant. 3D braid preforms: 0°- and 45°-direction specimens had higher initial elastic modules (0.018 GPa and 0.015 GPa, respectively) and yield stresses (0.42 MPa and 0.28 MPa, respectively) than Z-direction specimens (0.007 GPa and 0.21 MPa, respectively).
Bagsik et al., 2011	Orientation toolpath generation	Ultem® 9085	Raster angles: 0°, 30°, 45° Raster-to-raster gap: +0.001, 0, -0.001 Perimeter to raster gap: 3 levels each Layer thickness: 2 levels	Negative raster air gap, thick layer thickness, X and Z direction yielded best tensile strength (84MPa).
Wu et al., 2015	Layer thickness and raster angle	PEEK and ABS P430	PEEK: custom 3D printer ABS P430: uPrint SE 3D printer	The tensile, compression and bending strengths of PEEK samples were higher than those of ABS samples by 108%, 114% and 115%, respectively.
Motaparti et al., 2016	Effect of processing parameters on compression properties	Ultem® 9085	Build direction: 0.508 mm Raster angle: 45°, -45° Air gap: 2.54 mm	Vertical build with 0°, 90° raster angle had 15 to 30% flexural strength, 15 to 40% compression test.
Zaldivar et al., 2017	Processing parameters and orientation	Ultem®	Flat 0°, flat 90°, edge, upright, edge 45°, flat 45°	X-orientation (0°) had tensile strength of 71.03MPa and 85.8% strength utilisation.

Xiaoyong et al., 2017	Temperature	PEEK and PLA	Temperature: 130°C, 110°C, 25°C, Filling ratio: 100%, 50%	Maximum tensile strength of PEEK was around 77Mpa, which was much larger than the tensile strength of PLA, and has good forming properties in thin layer parts.
Deng et al., 2018	Mechanical properties	PEEK	Printing speed: 20, 40, 60 Layer thickness: 0.2, 0.25, 0.30 Printing temperature: 350°C, 360°C, 370°C Filing ratio: 20, 40, 60	PEEK specimens had optimal tensile properties at a printing speed of 60 mm/s, layer thickness of 0.2 mm, temperature of 370°C and filling ratio of 40%. Tensile strength was 40MPa, Young's modulus was 522.9MPa, and elongation was 14.3%.
Knoop et al., 2015	Mechanical properties	PA12	Orientation: X, Y, Z	X-direction had highest tensile strength (55MPa).
Verdejo et al., 2020	compression modulus	Short carbon fibre reinforced PA6	manufactured using FDM and polymer injection moulding (PIM) methods	The compression modulus of the FDM printed fibre composite and injection moulded composite was 3931 MPa and 1950 MPa, respectively.
Gavali et al., 2019	Mechanical and thermomechanical properties	PLA and CF	Studied by varying the percentage of 12%, 15% and 20% of chopped carbon fiber	6.11 kJ/m^2 reduction of the absorbed energy (87%) by the 20 wt% CF composite as compared to the pure ASA. PLA 20 wt% of CF Notched 6.11 kJ/ m2 Increment of impact strength was observed when the CF content increased from 15 wt% to 20 wt%.
Wang et al., 2020		PEEK and short carbon fibre (average length of 205 μm) and glass fibre (average length of 96 μm)	fibre reinforcements of 5, 10, and 15 wt%	Glass fibre composites exhibited better thermal stability than the carbon fibre composites due to enhanced interfacial bonding. A minimum weight loss of 43% was noted for 10 wt% glass fibre composites, while for 10 wt% carbon fibre composite the same was 47%. An increase in the melting point, thermal decomposition temperature, and crystallisation temperature was noted on the composites when increasing the fibre content

Gavali et al., 2020	flexural strength	PLA and CCF composite	PLA and varying 10%, 12% and 15% CCF composite.	The PLA exhibited flexural strength of 66 MPa and on reinforcing 10 wt% of carbon fibre, the strength increased to 67 MPa. When the weight percentage increased to 15%, the flexural strength was ca. about 78 MPa
Pertuz et al., 2020	tensile strength	PA composite with carbon, kevlar, and glass fibre reinforcements	The composites were printed at varying orientations 0°, 45°, and 60°.	Carbon fibre composites with 0 ◦ fibre orientation displayed a maximum tensile strength of 165 MPa.

3.0 TRIBOLOGICAL PROPERTIES

Friction and wear are mechanisms that remove material from solid surfaces via contact and sliding. As polymers generally offer low frictional resistance when sliding, they are frequently used in dry sliding conditions and provide better understanding when compared to wet conditions. Failure to consider tribological interactions as well as a lack of information has significantly contributed to the poor performance of high-end machine parts and a waste of resources. Therefore, the extensive use of polymers in final products has motivated researchers to investigate the fundamental mechanisms of friction and wear in polymers (Dearn et al., 2013; Franklin et al., 2001; Jia et al., 2007)

The tribological properties of 3D-printed polymer components are generally improved when using optimal printing parameters (Gurrala and Regalla, 2014; Garg at al., 2015; Norani et al., 2020), incorporating surface modifications such as filament-reinforced carbon materials (Pawlak., 2018) and taking into account filament temperature and colour (Hanon et al., 2019).

Gurrala and Regalla (2014) explored the friction and wear behaviour of ABS polymer parts made of FFF. They considered the effect of three parameters: 1) load, 2) speed, and 3) orientation using FCCCD on the wear rate and friction coefficient of FFF parts. Sliding speed affects friction more than orientation at a fixed load. The parts produced via FFF have asperities, however, as the surface roughness smoothes out over time, the coefficient of friction (COF) decreases and becomes stable as most of the material is worn out in the form of powder. Damage to contact surfaces is usually caused by wear patterns; such as abrasion, tiredness, ploughing, corrugation, erosion and cavitation. Abrasive wear often results in irreversible changes to the contours of the body due to changes in the gaps between the solids that are in contact. Wear rate will usually jump from a minimum value to a value at which it stabilises and obey a fixed linear rate.

A study of the wear and COF of PLA-graphite composites in 3D printing technology by Pawlak (2018) found that PLA had a higher wear rate and COF; 15.2μm/km and 0.492, respectively; than 50% PLA-graphite (15.2μm/km and 0.288). As such, the 50% PLA-graphite was much more brittle and caused difficulties upon dosing the filament.

Norani et al., (2020) attempted to determine the most optimal 3D printing parameters by analysing the friction and wear coefficient properties of an ABS polymer using the response surface methodology (Box–Behnken Design). The study found that layer height significantly affected the COF and wear rate. It was discovered that a layer height of 0.10 mm, a nozzle

temperature of 234°C, and using a triangle printing pattern were the most optimal parameters to minimise COF (0.2788) and wear rate (2.1136 10^{-4} mm^3/N m).

Garg et al., (2015) compared the wear behaviour of an ABS part with a Nylon6−Fe powder composite part prepared via FDM. ABS was found to have a higher COF (0.35μ) than the Nylon6-Fe composite (0.26μ). It was also noted that the μ decreased as the load increased. The resistance friction forces presented through the bodies under sliding conditions. At the beginning of the friction tests, the frictional force was found to be higher before it slowly decreased and stagnated. This was due to the formation of transition layers on the sliding surface. Therefore, it can be concluded that speed greatly impacts wear resistance and can be useful in anti-wear applications. The wear of the ABS (0.15g) was much higher than that of the composite (0.01g). The Nylon6-Fe composite had a much lesser loss of mass which indicates that it has a very high wear resistance. This can be attributed to the presence of Fe in the composite. The wear that did occur was due to a combination of abrasion and adhesion. Therefore, the higher wear occurred at higher sliding velocities. This was the true for both the ABS material and the composite material.

Hanon et al., (2019) examined the tribological behaviour of ABS and PLA polymers that had been 3D-printed with different colours at various printing temperatures (low, optimum, and maximum). The operating ranges and failure modes of the 3D-printed polymer samples were determined at regular and overload conditions. The dynamic friction coefficient results of the ABS specimen (0.27) were lower than the PLA specimen at all three temperature ranges. The 3D-printed PLA specimen was tested with various settings; which found some inconsistencies; however, the use of different colours showed a clear dissimilarity.

Studies indicate that it is vital to improve the tribological performance of 3D-printed ABS components and traditional manufacturing processes (Amiruddin et al., 2019; Hanon et al., 2019). Both studies found that 3D-printed ABS had higher COF values and wear rates. Amiruddin et al., (2019) concluded that intrinsic micro-sized hollow spaces inside the samples were caused by 100% infill which improved fluid absorption capacity as 3D-printed samples had an absorption rate that was two to four times greater than moulded ABS samples. Elsner et al., (2010) suggest that this higher absorption rate will facilitate micro-elastohydrodynamic lubrication (EHL) as well as cushion bearing capacity. Nonetheless, due to breaks or ruptures in the asperity surface finish, 3D-printed ABS had higher COF (0.040 to 0.055) and caused an increase in the actual contact area. This led to an increase in temperature and a decrease in the strength of the material resulting in an increase in friction. The main mechanisms of wearing in polymers and their composites is abrasive wear (Dawoud et al., 2015). As the wear progresses, the surface asperities are likely to compress and reduce the wear effect on the initial surface conditions and provide a more stable wear rate. Simultaneously, an increase in load will smooth the sliding surfaces through plastic deformation and breakage of asperity. This is likely to increase adhesive wear and decrease the wear rate as the sliding surfaces become smoother.

Hanon et al., (2019) compared the tribological behaviour of ABS polymers manufactured via turning and 3D printing. They found that the dynamic friction coefficient of turning manufactured ABS (0.257) was lower than 3D-printed ABS (0.266) while the wear levels of 3D-printed ABS (0.411 mm) was lower than turning manufactured ABS (0.442 mm). The adhesion wear mechanism on the turned surface changed to smooth and stronger at the beginning of the test than in the 3D-printed surface even though the surface pressure of the printed surface was smaller than the turned surface.

Apart from these methods, other studies have concluded that the implementation of internal/inner structures signify a significant reduction in friction and wear (Tahir et al., 2018;

Murashima et al., 2017; Abdollah et al., 2020; Norani et al., 2020). These studies also found that the lowest COF in inner structures was around 0.34 compared to the unstructured COF (No Hole) 3D-printed pin (0.71). The lowest wear rate (6.5 x 10^{-4} mm^3/Nm) was found in inner structures Hole A (2mm) (Tahir et al., 2018). Murashima et al., (2017) explains that the presence of internal structures produces a small and apparent of Young's modulus which increases the contact area. In other words, a small contact area under sliding increases the surface temperature more than a large contact area under sliding (Lim and Ashby, 1987) which affects the friction in polymer materials (Grosch et al., 1963). This mechanism could be considered for decreasing surface temperatures and friction coefficients.

Abdollah et al., (2020) investigated the dry sliding behaviour of ABS pins that had been 3D-printed with different internal geometries under varying normal loads and sliding speeds. The result showed that, at testing conditions of 58.68 N and 800 rpm, pins with a triangular flip internal structure had a minimum COF (0.27) value and wear rate (2.7 × 10^{-5} mm^3/Nm). This indicates that wear rate and COF values are relatively dependent on the normal loads, sliding speeds, and internal geometries. Triangle flip internal structures had lower maximum stresses distributed on the contact surface while there was no statistically significant correlation between the tribological and mechanical properties of ABS pins that had been 3D-printed with different internal geometries. Delamination, abrasion, and lower fatigue wear were seen as the main wear mechanisms that caused mild and serious wear.

As inclined or curved contact is intertwined between two surfaces, ploughing takes place during the sliding process (Kato et al., 2001) which removes a certain volume of material from the surface and results in the formation of a groove in the weaker surface. A single sliding pass does not generate wear particles in the ploughing mode and only results in a shallow groove. Repetitive sliding as well as the accumulation of plastic flow on the surface are required to generate wear particles. Delamination, which occurs when layers of material are separated from the surface of the bulk material, is thought to arise as a consequence of plastic deformation, high stress and the initiation of subsurface cracking. ABS pins that had been 3D-printed with an internal triangular flip structure were found to have the most favourable shortest run-in period and the lowest COF with high wear resistance. Research map and additional findings on 3D-printed polymer parts' tribological properties are tabulated in Figure 3 and Table 3, respectively.

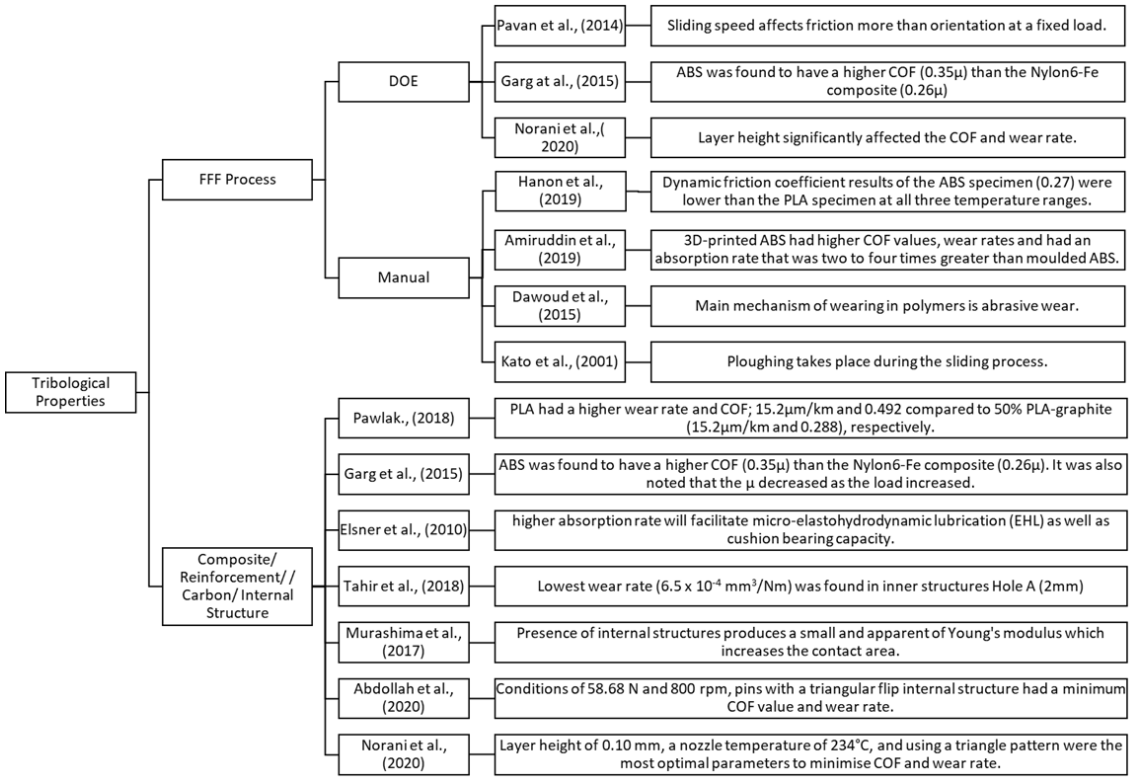

Figure 3: Research map (tribological properties).

Table 3: Summary of studies on the tribological properties of polymers.

Authors	Research Objective	Polymer Materials	Methods	Findings
Panin et al., 2019	Different solid lubricant filler loads on mechanical and tribotechnical properties under dry sliding friction conditions	PEEK loaded with organic PTFE and molybdenum disulphide (MoS_2) microparticles	Different filler loads were tested using Pin-on-disk with (10 N) load and V (0.3m/s) sliding velocity The use of metal and ceramic balls was tribotechnically tested: PEEK, PEEK + 10 wt % PTFE, PEEK + 1 wt % MoS_2, PEEK + 10 wt	PTFE was found to be an effective solid PEEK matrix lubricant (the wear resistance of the composite increased by 8 times with metal-polymer tribo-pair while it enlarged by 15 times with ceramic-polymer). When the content of the former does not exceed 0.5 wt % loading of MoS_2 together with PTFE microparticles ensures maximum wear resistance of the composite to maintain the basic strength properties at the level of the neat polymer. PEEK + 10 wt % PTFE + 0.5 wt % PTFE + 0.5 wt % MoS_2 is recommended as an effective antifriction

			% PTFE + 0.5 wt % MoS_2 Traveling distance: 3 km	material for use as a friction unit component for both metal polymer and ceramic polymer friction units.
Dangnan et al., 2020	Effect of varying contact loads on friction and wear	ABS and VeroGray™ polymers	Loads of 1, 5 and 10 N were applied under dry sliding contact with a 52100-steel counter face at room temperature	At 1 N load, the frictional performance was shown to be strongly (1.2) dependent on the 3D ABS surface with perpendicular orientation, where surface asperities during the reciprocating sliding were seen to play a major role. However, at higher loads; 5 and 10 N; the mechanical properties of the bulk affected COF to a greater degree than surface roughness.
Sable et al., 2020	Yield strength and friction phenomena at high strain-rate using uniaxial and oblique impact configurations	PU and epoxy	Impact velocities: 50 to 120 m/s for oblique Up to 1200 m/s for uniaxial	At a high strain rate, the COF for both polymers was found to be inversely proportional to pressure. For PU and epoxy, respectively, minimum values of 0.11 and 0.26 were measured under maximum pressure. Pressure dependency of shear strength persisted at high strain-rate for both PU and epoxy.
Marathe et al., 2020	Performance and tribological properties	50 wt % PEEK, 30 wt % 3 mm (GF), and 20 wt % synthetic graphite	Injection moulding (I) and compression moulding (C)	Final fibre length of 200–300 μm and 1.5 mm were observed for I and C composites, respectively, based on thermal degradation of composites at 600°C. Low specific wear rate (K0) (~10-16 m3/Nm) and friction coefficient (μ) (~0.03–0.05) were observed in both composites. Similarly, ~10-10 m3 /Nm and ~0.5–0.7, correspondingly, were observed for abrasive wear, K0 and μ. In both cases, the μ of the I composite was smaller. The C composite was superior to the I composite in adhesive wear efficiency, but not in abrasive wear.

Rathaur et al., 2019	Mechanical and tribological characterisation	Epoxy resin blended with graphite/talc micro fillers	Epoxy resin blended with graphite/talc micro fillers for 15 minutes at a constant speed of 1200 rpm and an applied load of 100 N as per the ASTM D4172 under dry conditions	Graphite (10 wt%) /talc (10 wt%)/epoxy demonstrated a significant reduction by ~63% (0.103 to 0.276) in COF and a moderate increment by ~34% in wear resistance in comparison to pure epoxy bearing balls under dry conditions. Hardness improved by ~5% in the graphite (10 wt%)/talc (10 wt%) /epoxy composite bearing ball.

4.0 CONCLUSIONS

The Fourth Industrial Revolution (or Industry 4.0) has increased the demand for technological breakthroughs in additive manufacturing (AM) as it is capable of increasing output and manufacturing high quality prints and complex components at a fractional of the cost. Therefore, this paper focused on literature exploring the effects of diverse process printing parameters, composite materials, internal geometries, lattices, and optimisation on the mechanical and tribological properties of polymer test specimens and their after effects. Although most of the studies analysed were mainly based on experimental data, some compared the mechanical and tribological properties of different polymers.

It was concluded that a minimum layer thickness, an orientation of zero, maximum raster angle and width, and negative air gap yields the highest mechanical strength. This indicates that while a polymer has high strength, it has low adhesion, plastic deformation, buckling, and weak interlayering which will generate thermal bonding towards itself. Although 3D-printed polymers have anisotropic porosity behaviours, its elasticities are better than its absorption capacity. In terms of tribological properties, 3D-printed polymers exhibit low friction and wear due to increased contact area, plastic deformation, and asperities breaks under specific sliding conditions. This is similar to findings by Aher et al., (2020) where the mechanism of wear and deterioration are abrasion, asperity break, ploughing, delamination, and cracking. Therefore, it is vital to the gather and understand information regarding the correlation between processing parameters and composite materials with the mechanical and tribological behaviour of 3D-printed FFF polymer specimens and components in order to accurately determine if these parts can meet the specific mechanical requirements for which they are produced.

In conclusion, the mechanical and tribological properties of 3D-printed polymers can satisfy the much-anticipated needs of users and manufacturers.

ACKNOWLEDGEMENT

The authors would like to extend their deepest gratitude and acknowledge the contributions of members of the Green Tribology and Engine Performance (G-TriboE) research group of Universiti Teknikal Malaysia Melaka. This research was supported by a grant from the Ministry of Higher Education Malaysia (Grant Number: FRGS/2018/FTKMP-CARE/F00385).

REFERENCES

Abdollah, M. F. B., Norani, M. N. M., Abdullah, M. I. H. C., Amiruddin, H., Ramli, F. R., & Tamaldin, N. (2020). Synergistic effect of loads and speeds on the dry sliding behaviour of fused filament fabrication 3D-printed acrylonitrile butadiene styrene pins with different internal geometries. The International Journal of Advanced Manufacturing Technology, 108(7), 2525-2539.

Aher, V. S., Shirsat, U. M., Wakchaure, V. D., & MA, V. (2020). An experimental investigation on tribological performance of UHMWPE composite under textured dry sliding conditions. Jurnal Tribologi, 24, 110-125.

Ahn, S. H., Montero, M., Odell, D., Roundy, S., & Wright, P. K. (2002). Anisotropic material properties of fused deposition modeling ABS. Rapid Prototyping Journal, 8(4), 248–57.

Amiruddin, H., Abdollah, M. F. B., & Norashid, N. A. (2019). Comparative study of the tribological behaviour of 3D-printed and moulded ABS under lubricated condition. Materials Research Express, 6(8), 085328.

Aslanzadeh, S., Saghlatoon, H., Honari, M. M., Mirzavand, R., Montemagno, C., & Mousavi, P. (2018). Investigation on electrical and mechanical properties of 3D printed nylon 6 for RF/microwave electronics applications. Additive Manufacturing, 21, 69-75.

ASTM52900-15 (2015). Standard terminology for additive manufacturing—general principles—terminology. ASTM International, West Conshohocken, PA, 3(4), 5.

Azmi M. S., Hasan R., Ismail R., Rosli N. A., & Alkahari M. R. (2018). Static and dynamic analysis of FFF printed lattice structures for sustainable lightweight material application. Progress in Industrial Ecology, 12(3), 247–259.

Bagsik. A., & Schoeppner. V. (2011). Mechanical properties of fused deposition modeling parts manufactured with Ultem 9085, Proceedings of the ANTEC, Plastics: Annual Technical Conference Proceedings, ANTEC.

Balderrama-Armendariz, C. O., MacDonald, E., Espalin, D., Cortes-Saenz, D., Wicker, R., & Maldonado-Macias, A. (2018). Torsion analysis of the anisotropic behavior of FDM technology. The International Journal of Advanced Manufacturing Technology, 96(1), 307-317.

Cantrell, J. T., Rohde, S., Damiani, D., Gurnani, R., DiSandro, L., Anton, J., Young. A., Jerez. A., Steinbach. D., Kroese. C., & Ifju, P. G. (2017). Experimental characterization of the mechanical properties of 3D-printed ABS and polycarbonate parts. Rapid Prototyping Journal, 23(4), 811-824.

Christiyan, K. J., Chandrasekhar, U., & Venkateswarlu, K. (2016, February). A study on the influence of process parameters on the Mechanical Properties of 3D printed ABS composite. In IOP Conference Series: Materials Science and Engineering (Vol. 114, No. 1, p. 012109). IOP Publishing.

Chua. C. K. & Leong, K. F. (2014). 3D printing and additive manufacturing: principles and applications. 4th ed. Singapore: World Scientific Publishers.

Chua. C. K. & Yeong. W. Y. (2015). Bioprinting: principles and applications. Singapore: World Scientific Publishing Co. Pte. Ltd.

Dangnan, F., Espejo, C., Liskiewicz, T., Gester, M., & Neville, A. (2020). Friction and wear of additive manufactured polymers in dry contact. Journal of Manufacturing Processes, 59, 238-247.

Dearn, K. D., Hoskins, T. J., Petrov, D. G., Reynolds, S. C., & Banks, R. (2013). Applications of dry film lubricants for polymer gears. Wear, 298, 99-108.

Deng, X., Zeng, Z., Peng, B., Yan, S., & Ke, W. (2018). Mechanical properties optimization of poly-ether-ether-ketone via fused deposition modeling. Materials, 11(2), 216.

Domínguez-Rodríguez, G., Ku-Herrera, J. J., & Hernández-Pérez, A. (2018). An assessment of the effect of printing orientation, density, and filler pattern on the compressive performance of 3D printed ABS structures by fuse deposition. The International Journal of Advanced Manufacturing Technology, 95(5), 1685-1695.

Es-Said, O. S., Foyos, J., Noorani, R., Mendelson, M., Marloth, R., & Pregger, B. A. (2000). Effect of layer orientation on mechanical properties of rapid prototyped samples. Materials and Manufacturing Processes, 15(1), 107-122.

Franklin, S. E. (2001). Wear experiments with selected engineering polymers and polymer composites under dry reciprocating sliding conditions. Wear, 251(1-12), 1591-1598.

Furtado, S. C. R., Silva, A. J., Alves, C., Reis, L., Freitas, M., & Ferrão, P. (2012). Natural fibre composites: automotive applications. In Natural polymers (pp. 118-139).

Galeta, T., Raos, P., Stojšić, J., & Pakši, I. (2016). Influence of structure on mechanical properties of 3D printed objects. Procedia Engineering, 149, 100-104.

Garg, H. K., & Singh, R. (2015). Comparison of wear behavior of ABS and Nylon6—Fe powder composite parts prepared with fused deposition modelling. Journal of Central South University, 22(10), 3705-3711.

Gavali, V. C., Kubade, P. R., & Kulkarni, H. B. (2020). Mechanical and thermo-mechanical properties of carbon fiber reinforced thermoplastic composite fabricated using fused deposition modeling method. Materials Today: Proceedings, 22, 1786-1795.

Gavali, V. C., Kubade, P. R., & Kulkarni, H. B. (2020). Property Enhancement of Carbon Fiber Reinforced Polymer Composites Prepared by Fused Deposition Modeling. Materials Today: Proceedings, 23, 221-229.

Gibson, L.J., & Ashby, M. F. (1999). Cellular solids: structure and properties, 2nd edition Cambridge University Press, Cambridge.

Grosch, K. A. (1963). The relation between the friction and visco-elastic properties of rubber. Proceedings of the Royal Society of London. Series A. Mathematical and Physical Sciences, 274(1356), 21-39.

Gurrala, P. K., & Regalla, S. P. (2014). Friction and wear behavior of abs polymer parts made by fused deposition modeling (FDM). Technology Letters, 1, 13-17.

Hager. I., Golonka. A., Putanowicz. R. (2016). 3D Printing of Buildings and Building Components Hager, I., Golonka, A., & Putanowicz, R. (2016). 3D printing of buildings and building components as the future of sustainable construction. Procedia Engineering, 151, 292-299.

Hanon, M. M., Kovács, M., & Zsidai, L. (2019). Tribology behaviour investigation of 3D printed polymers. International Review of Applied Sciences and Engineering, 10(2), 173-181.

Hanon, S. M. M., Kovács, M., & Zsidai, L. (2019). Tribological Behaviour Comparison of ABS Polymer Manufactured Using Turning and 3D Printing. International Journal of Engineering and Management Sciences, 4(1), 46-57.

Huang, S. H., Liu, P., Mokasdar, A., & Hou, L. (2013). Additive manufacturing and its societal impact: a literature review. The International Journal of Advanced Manufacturing Technology, 67(5), 1191-1203.

Hull, C. W. (1984). Apparatus for production of three-dimensional objects by stereolithography. United States Patent, Appl., No. 638905.

Jasiuk, I., Abueidda, D. W., Kozuch, C., Pang, S., Su, F. Y., & McKittrick, J. (2018). An overview on additive manufacturing of polymers. JOM, 70(3), 275-283.

Jia, B. B., Li, T. S., Liu, X. J., & Cong, P. H. (2007). Tribological behaviors of several polymer–polymer sliding combinations under dry friction and oil-lubricated conditions. Wear, 262(11-12), 1353-1359.

Kabir, M. M., Wang, H., Lau, K. T., & Cardona, F. (2012). Chemical treatments on plant-based natural fibre reinforced polymer composites: An overview. Composites Part B: Engineering, 43(7), 2883-2892.

Kato, K., & Adachi, K. (2000). Wear mechanisms. In Modern Tribology Handbook: Volume One: Principles of Tribology (pp. 273-300). CRC press.

Kim, H., Park, E., Kim, S., Park, B., Kim, N., & Lee, S. (2017). Experimental study on mechanical properties of single-and dual-material 3D printed products. Procedia Manufacturing, 10, 887-897.

Knoop, F., Schoeppner, V., Knoop, F. C., & Schoeppner, V. (2015, August). Mechanical and thermal properties of FDM parts manufactured with polyamide 12. In Proceedings of the 26th Annual International Solid Freeform Fabrication Symposium—An Additive Manufacturing Conference, Austin, TX, USA (pp. 10-12).

Lee, C. S., Kim, S. G., Kim, H. J., & Ahn, S. H. (2007). Measurement of anisotropic compressive strength of rapid prototyping parts. Journal of materials processing technology, 187, 627-630.

Leite, M., Varanda, A., Ribeiro, A. R., Silva, A., & Vaz, M. F. (2018). Mechanical properties and water absorption of surface modified ABS 3D printed by fused deposition modelling. Rapid Prototyping Journal, 24(1), 195–203.

Lim, S. C., & Ashby, M. F. (1987). Overview no. 55 wear-mechanism maps. Acta Metallurgica, 35(1), 1-24.

Lovo, J. F. P., Camargo, I. L. D., Araujo, L. A. O., & Fortulan, C. A. (2020). Mechanical structural design based on additive manufacturing and internal reinforcement. Proceedings of the Institution of Mechanical Engineers, Part C: Journal of Mechanical Engineering Science, 234(2), 417-426.

Maeda, H., Okubo, H., & Sasaki, S. (2019). Frictional property of a 3D-capillary-structured surface fabricated by selective laser melting. Jurnal Tribologi, 20, 87-96.

Marathe, U. N., & Bijwe, J. (2020). High performance polymer composites-influence of processing technique on the fiber length and performance properties. Wear, 446, 203189.

Mohamed, O. A., Masood, S. H., & Bhowmik, J. L. (2015). Optimization of fused deposition modeling process parameters: a review of current research and future prospects. Advances in Manufacturing, 3(1), 42-53.

Morocho, J. R., Sánchez, A. C., Singaña, M., & Donoso, C. (2020). Effect of the Filling Pattern on the Compression strength of 3D Printed Objects Using Acrylonitrile Butadiene Styrene (ABS). Key Engineering Materials, 834, 115-119.

Motaparti, K. P. (2016). Effect of build parameters on mechanical properties of ultem 9085 parts by fused deposition modeling. Master Thesis, Missouri University of Science and Technology.

Murashima, M., Kawaguchi, M., Tanaka, M., & Umehara, N. (2017). The effect of inner structures created by 3D-additive manufacturing on wear reduction of 3D printed material. Proceedings of SAKURA Symposium on Mechanical Science and Engineering, 39-41.

Murphy, S. V. & Atala, A. (2014). 3D bioprinting of tissues and organs. Nature Biotechnology. 32, 773–785.

Mutalib, M. Z. A., Ismail, M. I. S., As' arry, A., & Jalil, N. A. A. (2020). Evaluation of tool wear and machining performance by analyzing vibration signal in friction drilling. Jurnal Tribologi, 24, 100-109.

Nor, S. M. M., Sudin, M. N., & Razali, M. F. B. (2018, August). Application of Taguchi method in investigating the effect of layer thickness and fill angle on FDM parts. In IOP Conference Series: Materials Science and Engineering (Vol. 409, No. 1, p. 012018). IOP Publishing.

Norani, M. N. M., Abdollah, M. F. B., Abdullah, M. I. H. C., Amiruddin, H., Ramli, F. R., & Tamaldin, N. (2020). Correlation of tribo-mechanical properties of internal geometry structures of fused filament fabrication 3D-printed acrylonitrile butadiene styrene. Industrial Lubrication and Tribology, 72(10), 1259-1265.

Norani, M. N. M., Abdollah, M. F. B., Abdullah, M. I. H. C., Amiruddin, H., Ramli, F. R., & Tamaldin, N. (2021). 3D printing parameters of acrylonitrile butadiene styrene polymer for friction and wear analysis using response surface methodology. Proceedings of the Institution of Mechanical Engineers, Part J: Journal of Engineering Tribology, 235(2), 468-477.

Onwubolu, G. C., & Rayegani, F. (2014). Characterization and optimization of mechanical properties of ABS parts manufactured by the fused deposition modelling process. International Journal of Manufacturing Engineering, 2014.

Panin, S. V., Nguyen, D. A., Kornienko, L. A., & Ivanova, L. R. (2019, November). Multicomponent antifriction composites based on polyetheretherketone (PEEK) matrix. In AIP Conference Proceedings (Vol. 2167, No. 1, p. 020267). AIP Publishing LLC.

Peças, P., Carvalho, H., Salman, H., & Leite, M. (2018). Natural fibre composites and their applications: a review. Journal of Composites Science, 2(4), 66.

Perepelkina, S., Makhmudova, K., & Kovalenko, P. (2020). Investigation of Mechanical Properties of Anisotropic Materials Used in Rapid Prototyping Technologies. Materials Science Forum, 989, 821-826.

Pertuz, A. D., Díaz-Cardona, S., & González-Estrada, O. A. (2020). Static and fatigue behaviour of continuous fibre reinforced thermoplastic composites manufactured by fused deposition modelling technique. International Journal of Fatigue, 130, 105275.

Prakash, K. S., Nancharaih, T., & Rao, V. S. (2018). Additive manufacturing techniques in manufacturing-an overview. Materials Today: Proceedings, 5(2), 3873-3882.

Quan, Z., Suhr, J., Yu, J., Qin, X., Cotton, C., Mirotznik, M., & Chou, T. W. (2018). Printing direction dependence of mechanical behavior of additively manufactured 3D preforms and composites. Composite Structures, 184, 917-923.

Rankouhi, B., Javadpour, S., Delfanian, F., & Letcher, T. (2016). Failure analysis and mechanical characterization of 3D printed ABS with respect to layer thickness and orientation. Journal of Failure Analysis and Prevention, 16(3), 467-481.

Rathaur, A. S., Patel, V. K., & Katiyar, J. K. (2019). Tribo-mechanical properties of graphite/talc modified polymer composite bearing balls. Materials Research Express, 7(1), 015305.

Sabahi, N., Chen, W., Wang, C. H., Kruzic, J. J., & Li, X. (2020). A review on additive manufacturing of shape-memory materials for biomedical applications. JOM, 72(3), 1229-1253.

Sable, P. A., Neel, C. H., & Borg, J. P. (2020). Dynamic strength and friction behavior of thermosetting polyurethane and epoxy. In AIP Conference Proceedings (Vol. 2272, No. 1, p. 040010). AIP Publishing LLC.

Samykano, M., Selvamani, S. K., Kadirgama, K., Ngui, W. K., Kanagaraj, G., & Sudhakar, K. (2019). Mechanical property of FDM printed ABS: Influence of printing parameters. The International Journal of Advanced Manufacturing Technology, 102(9), 2779-2796.

Seidl, M., Šafka, J., Bobek, J., Běhálek, L., & Habr, J. (2017). Mechanical properties of products made of abs with respect to individuality of fdm production processes. Modern Machinery Science Journal, 2, 1748-1751.

Seliktar, D., Dikovsky, D., & Napadensky, E. (2013). Bioprinting and tissue engineering: recent advances and future perspectives. Israel Journal of Chemistry, 53(9-10), 795-804.

Soffie, S. M., Ismail, I., Nurain, M. A., Aqida, S. N., & Pekan, P. (2020). The morphological and surface roughness of magnetorheological polished AISI 6010 surface. Jurnal Tribologi, 24, 80-99.

Sood, A. K., Ohdar, R. K., & Mahapatra, S. S. (2010). Parametric appraisal of mechanical property of fused deposition modelling processed parts. Materials & Design, 31(1), 287-295.

Sreenivasan, S., Sulaiman, S., Baharudin, B. T. H. T., Ariffin, M. K. A., & Abdan, K. (2013). Recent developments of kenaf fibre reinforced thermoset composites. Materials Research Innovations, 17(sup2), s2-s11.

Tahir, N. A. M., Azmi, M. S., Abdollah, M. F. B., Ramli, F. R., Amiruddin, H., Tokoroyama, T., & Umehara, N. (2018). Tribological properties of 3D-printed pin with internal structure formation under dry sliding conditions. Proceedings of Mechanical Engineering Research Day, 2018, 260-261.

Tibbits, S. (2013). The emergence of "4D printing". In TED conference.

Tymrak, B. M., Kreiger, M., & Pearce, J. M. (2014). Mechanical properties of components fabricated with open-source 3-D printers under realistic environmental conditions. Materials & Design, 58, 242-246.

Uddin, M. S., Sidek, M. F. R., Faizal, M. A., Ghomashchi, R., & Pramanik, A. (2017). Evaluating mechanical properties and failure mechanisms of fused deposition modeling acrylonitrile butadiene styrene parts. Journal of Manufacturing Science and Engineering, 139(8), 081018.

Verdejo de Toro, E., Coello Sobrino, J., Martínez Martínez, A., Miguel Eguía, V., & Ayllón Pérez, J. (2020). Investigation of a short carbon fibre-reinforced polyamide and comparison of two manufacturing processes: Fused Deposition Modelling (FDM) and polymer injection moulding (PIM). Materials, 13(3), 672.

Wang, P., Zou, B., Ding, S., Huang, C., Shi, Z., Ma, Y., & Yao, P. (2020). Preparation of short CF/GF reinforced PEEK composite filaments and their comprehensive properties evaluation for FDM-3D printing. Composites Part B: Engineering, 198, 108175.

Wu, W., Geng, P., Li, G., Zhao, D., Zhang, H., & Zhao, J. (2015). Influence of layer thickness and raster angle on the mechanical properties of 3D-printed PEEK and a comparative mechanical study between PEEK and ABS. Materials, 8(9), 5834-5846.

Xiaoyong, S., Liangcheng, C., Honglin, M., Peng, G., Zhanwei, B., & Cheng, L. (2017, January). Experimental analysis of high temperature PEEK materials on 3D printing test. In 2017 9th International conference on measuring technology and mechatronics automation (ICMTMA) (pp. 13-16). IEEE.

Zaldivar, R. J., Witkin, D. B., McLouth, T., Patel, D. N., Schmitt, K., & Nokes, J. P. (2017). Influence of processing and orientation print effects on the mechanical and thermal behavior of 3D-Printed ULTEM® 9085 Material. Additive Manufacturing, 13, 71-80.